AJBAR Vol 1(5), 2022: 80-102, ISSN: 2811-2881

Arid Zone Journal of Basic and Applied Research

Faculty of Science, Borno State University Maiduguri, Nigeria

Journal homepage: https://www.azjournalbar.com

Research Article

Adsorption of Pb (II) ion onto Modified Doum Palm (*Hyphaene thebaica*) Shells: Isotherm, Kinetic and Thermodynamic Studies

Alkali, M.I., [2]Abdus-Salam, N., [3]Dikwa, M.K., [4]Oyewumi-Musa, R.T., [5]Jimoh, A.A., [2]Ojo, I. and [6]John, G.

[1]Department of Chemistry, Borno State University, Maiduguri-Nigeria.
[2]Department of Chemistry, University of Ilorin, Nigeria.
[3]Department of Chemistry, University of Maiduguri, Nigeria.
[4]Department of Chemical and Geological, Al-Hikimah University, Nigeria
[5]Department of Chemistry, Kwara State University, Malete-Nigeria.
[6]Kogi State College of Education, (Technical), Kabba-Nigeria.
*Corresponding author: ibrambnanabe@gmail.com, doi.org/10.55639/607gfedc

ARTICLE INFO:

Keyword:
Adsorption,
Doum palm shell,
Lead,
Isotherm
Kinetic
Thermodynamics

ABSTRACT

The negative impact of high concentrations of lead in the analytical environment on humans and aquatic plants prompted this research. The adsorption of hazardous lead from an aqueous medium using a Modified Doum Palm (MDP) shell was investigated. The modification of the Doum palm shell was supported via 2 M 1: 2 $ZnCl_2$ as activating agent. The batch equilibrium technique was employed to study the effect of initial concentration (800 mg/L), contact time (90 min) and temperature (313 K) on the adsorption capacity of the prepared adsorbent. Experimental data were analyzed using four kinetic models: pseudo-first-order, pseudo-second-order, intra-particle diffusion and Elovich models and it was found that the pseudo-second-order model fitted the adsorption data most with the highest correlation (R^2 = 0.9875). The studies of thermodynamic behaviour revealed negative values for ΔG^o (-26.7036 to -28.1252 kJ/mol), and negative values for ΔH^o (-15.5796 kJ/mol) and ΔS^o (0.03554 kJ/mol/k) respectively. These indicated the adsorption process was exothermic, feasible and spontaneous in the removal of the Pb (II) ion. The findings demonstrated that the adsorbent could be exploited in the removal of Pb (II) ion from an aqueous solution

Corresponding author: Alkali, M.I, Email: ibrambnanabe@gmail.com
Department of Chemistry, Borno State University, Maiduguri-Nigeria.

INTRODUCTION

Environmental pollution with heavy metals is a serious challenge worldwide posing peril to humans, animals, plants and the stability of the overall ecosystem. To address this problem, various water purification technologies have been adopted in many scientific research fields. Among the various concepts proposed, adsorption-based water treatment technologies are promising because of their large surface area, high aspect ratio, greater chemical reactivity, lower cost and energy, less chemical mass and impact on the analytical environment (Song *et al*., 2016).

However, adsorption has been reported for its worthy economical, as one of the most effective aqueous pollutant removals with low-cost or readily available activated carbon, simple in handling, low reagent consumption, unique and attractive as well as easy recovery through generation and desorption of adsorbents (Adekola *et al*., 2012; Akinyeye *et al*., 2020).

Pb (II) ion is one of the most toxic and long-existing environmental pollutants (WHO, 2016; EPA, 2021). Many chemical industries such as textile, metal plating, printing, finishing and tanning, glass industry, and battery manufacturing generate a huge amount of wastewater contaminated with Pb (II) ions in drinking and wastewater are 0.015 mg/L and 0.005 mg/L respectively (Tóth *et al*., 2016; Ombugus *et al*., 2021). Pb (II) ions can affect almost all the vital organs in human, animal and plant anatomy (Wang *et al*., 2019). Exposure of Pb (II) ions above the permissible limit may cause severe damage to the vital organs and eventually cause death to the affected organism (Ayob *et al*., 2021). Hence, the removal of this dangerous metal ion is paramount in the analytical research field to protect animals, plants and aquatic organisms.

Doum palm (*Hyphaene thebaica*) Hyphaene is derived from the Greek word 'hyphaino' referring to the fibres from the leaves, which are used for weaving. Its common names are Dom (Arabic), doum palm, Egyptian doum palm, gingerbread palm (English) and Goruba (Hausa). The plant is native to Nigeria, Niger, Benin, Burkina Faso, Cameroon, Senegal, Sierra Leone and Sudan (Abu-Elalla, 2009).

The mesocarp (pulp) of the fruits of *H. thebaica* was found to contain 12.65 % ash, 89.25 % carbohydrate, 0.95 % oil, 316 mg/g glucose, the very low protein content of 0.01 % and calorific values of 3655.9 kcal/kg. The anti-nutritional factor, tannin, the content was 8.30 mg/g. It also contains Ca (245.10 mg/100 g), Mg (236.45 mg/100 g), Fe (47.96 mg/100 g), Cu (0.38) and Zn (0.62). The mineral concentrations in the mesocarp seem to be adequate to provide livestock with the required metal essential for biochemical activities (Salih, 1991; Nwosu *et al*., 2008). Apart from the nutritional values of the doum palm, the shells are in abundance, thus polluting the environment.

Fig. 1: Doum palm Shells (*Hyphaene thebaica*)

The combination of physical and chemical activation processes leads to the production of activated carbon with a specific surface area. Chemical activation involves the impregnation of Doum palm shells with zinc chloride as an activating agent to improve the surface area, reduce the formation of tar and significantly increase carbon yield (Adebayo *et al*., 2014).

Therefore, it is obvious to design a feasible method to reduce the pollution caused by Pb (II) ion discharge and reduce the dangers joined with its presence in the analytical environment (Dada *et al*., 2012). This study aims to evaluate the adsorption of Pb (II) ion from an aqueous medium using a modified Doum palm shell and use the data obtained will be also to evaluate equilibrium isotherm, kinetics and thermodynamic studies.

MATERIALS AND METHODS

Sample Collection

The Doum palm shells (*Hyphaene thebaica*) were harvested from the plant within Mobbar local Government area of Borno State, North Eastern region of Nigeria which was located between latitude 13.1330˚ N and longitude 12.7135˚E and transported to the laboratory for preliminary treatment before use. The sample was washed thoroughly with tap water, followed by washing with deionized water and finally dried in an oven for 48 hrs at 70 °C.

Reagents and Instruments

All chemicals used are analytical-grade reagents. $Pb(NO_3)_2$ (99.5 %), NaOH (pellets), HNO_3 (65 %), H_2SO_4 (97 %), $ZnCl_2$ (98 %), KOH (95 %) were purchased from Sigma-Aldrich, Iran.

The main instruments used during the study are a pH meter equipped with a combined glass-saturated calomel electrode calibrated with buffer solutions of pH 4.0, 7.0 and 9.2, Fourier-Transform Infrared Spectroscopy (FTIR) spectrophotometer (SHIMADZU 8400S model), Atomic Absorption Spectrophotometer (AAS) (210VGP model), Scanning Electron Microscopy (SEM) (Tescan MIRA 3) and Energy Dispersive X-ray (EDX) (FEI model operating at 20 KV) respectively.

Modification of Doum palm Shells

The preparation of modified Doum palm (*Hyphaene thebaica*) shells involved chemical activation and washing. A 20 g of the dried Doum palm shells was impregnated with a 3M concentration of $ZnCl_2$ as activating agent at 1:2 and the solution was kept for 24 hrs at room temperature before further analysis (Abdus-Salam and Ikudayisi, 2017).

$$\text{Impregnation ratio} = \frac{weight\ of\ the\ activating\ agent}{weight\ of\ the\ carbonizing\ material} \quad (1)$$

This was followed by washing the samples severally with deionized water until neutral pH was obtained (Mahdavian, 2012; Ltifi *et al.*, 2017). The chemically activated sample was dried in an oven at 105 ^{o}C for 1 hr. The dried samples were weighed and taken into pyrolyser in a porcelain crucible to carbonize at 550 ^{o}C for 1 hr under N2 gas after which the sample was transferred into a desiccator to cool. The chemically activated carbon prepared was weighed to determine the percentage carbon yield Eq. 1 (Abdus-Salam and Ikudayisi, 2017).

The activated sample was ground into fine particle size using a mortar pestle and then sieved to 0.01 mm using a sieve. Finally, the sieved-activated samples were kept in a polyethylene bottle for an adsorption study (Abdus-Salam and Buhari, 2014; Adebayo *et al.*, 2014). The adsorbed quantity was calculated from eq. 2.

Batch Adsorption Experiment

The adsorption of Pb (II) ion unto modified Doum palm shell (MDP) was studied via batch experiments. A 0.01 g of adsorbent was shaken with 20mL Pb (II) ion concentration in a

thermostated shaker with a constant agitation speed of 230 rpm for 5 hrs. The optimization for the adsorption of Pb (II) ion onto modified doum palm shell was achieved by varying the different components such as adsorbent dosage, contact time, pH and equilibration of temperature. When the equilibrium was obtained, the samples were withdrawn from the shaker and supernatant liquids were filtered using filter paper. The residual Pb (II) ion concentration of each sample was measured using atomic absorption spectrophotometer. The amount of quantity adsorbed mg/g) of Pb (II) ion was calculated using the formulae reported by (Nwosu *et al*., 2017).

$$q_e = \frac{\mathrm{v}(\mathrm{c_i} - \mathrm{c_e})}{\mathrm{M}} \times 10^{-3} \quad (2)$$

where qe = is the amount of Pb (II) ion adsorbed from the solution in (mg/g) at equilibrium, Ci = the concentration before adsorption (mg/L), Ce = the concentration after adsorption (mg/L), V = volume of the adsorbate (L), and M = is the weight in a gram of the adsorbent (g) respectively (Abdus-Salam and Bello, 2015). The extent of adsorption was calculated using the eq. 3.

$$\%\ \text{Adsorption} = \frac{\mathrm{c_i} - \mathrm{c_e}}{\mathrm{c_i}} \times \frac{100}{1} \quad (3)$$

RESULTS AND DISCUSSION

Characterization Analysis

Scanning Electron Microscope (SEM)

Scanning Electron Microscopy is a useful analytical tool for visual confirmation of surface morphology and the physical state of the surface (Ghasemi *et al*., 2014). The SEM micrograph of MDP was presented in Fig. 2. It can be seen that MDP shells showed highly heterogeneous porous structures. Interestingly, this could be attributed to the beauty of $ZnCl_2$ in the modification of the adsorbent (Gaya *et al*., 2015). Meanwhile, the scanning electronic microscopy in conjunction with energy dispersive X-ray (EDX) analysis gives information on the chemical characterization of the activated carbon (Mafra *et al*., 2013). The summary of the EDX results was presented in Table 1. The results obtained are presented in the following order; 83.58 % (C) > 14.92 % (O) > 0.73 % (K) > 0.59 % (Si) > 0.18 % (Zn) respectively.

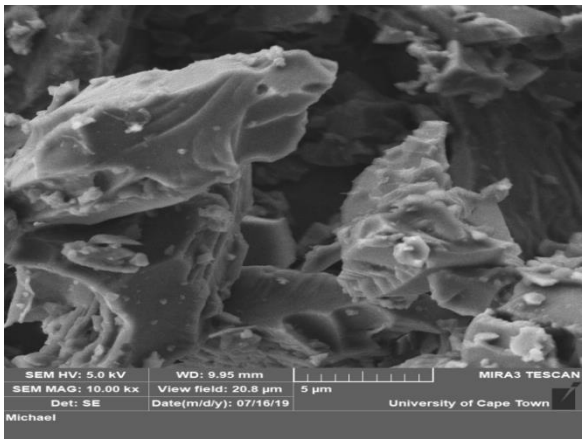

Figure 2: SEM Micrograph of MDP Shells

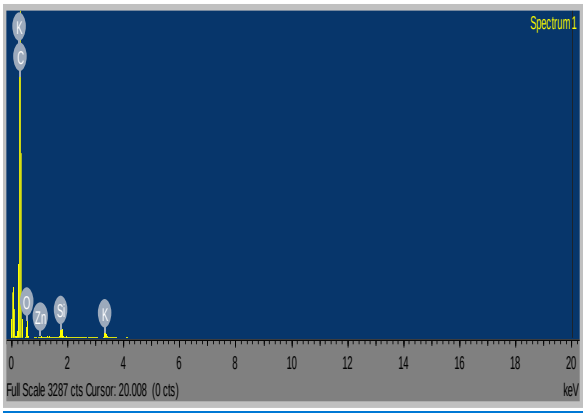

Figure 3: EDX Spectrum of MDP

Table 1: Summary of Elemental Composition of the Sample

Sample Code	C	O	K	Si	Zn	Total (%)
MDP	83.58	14.92	0.73	0.59	0.18	100

Fourier Transform Infrared Spectra (FTIR)

The FTIR technique is an important analytical tool used for identification of characteristic functional groups which take part in the chemistry of adsorption (Adegoke *et al*., 2014). The FTIR spectrum of MDP was depicted in Fig.4. The spectrum displays prominent sharp peaks. The intense absorption bands at 3412.19 cm^{-1} were attributed to the stretching vibration of –OH (Dada *et al*., 2016). The adsorption peak at 2920.32 cm^{-1} represented the stretching vibrations of –CH and $–CH_2$ (Adegoke *et al*., (2017). The peak observed at 1593.24 cm^{-1} was due to the –COOH and the peak observed near 1375.29 cm^{-1} was connected with phenol (Nyijime *et al*., 2021). The characteristic peak at 889.92 cm^{-1} could be ascribed to the C–O bending vibration in –COH (Abdus-Salam and Adekola, 2018). The band at around 752.26 cm^{-1} was related with the out of plane bending mode of O–H (Dada *et al*., 2018). Overall, the surface of MDP was rich in functional groups, especially for –OH, –COOH, and –COH. The

main functional groups, i.e. –OH, –COOH, and –COH, were polar functional groups, which can promote the adsorption of polar solute. The presence of these functional groups and their enhancement in adsorption abilities of MDP agrees with the findings of (Adegoke *et al*., 2017).

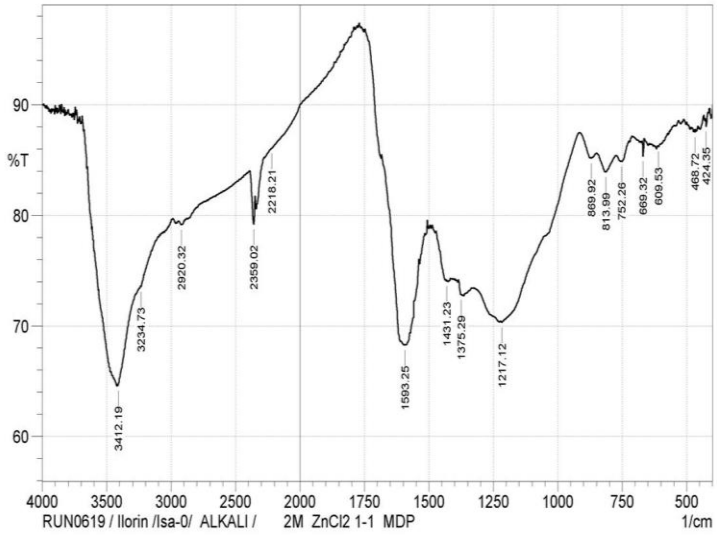

Figure 4: FT-IR spectrum of MDP Shells

BATCH ADSORPTION EXPERIMENT

Effect of the Initial Concentration

The effect of initial adsorbate concentration is an important component in adsorption studies because it provides in-depth information on the optimum concentration of aqueous solution required to saturate the active sites on the adsorbents (Abdus-Salam *et al*., 2021a). The plot of the initial metal ion concentration of Pb (II) ion on MDP was presented in Fig. 5. The initial adsorbate concentration on the MDP was determined by varying the concentrations; 1000 -200 mg/L.

The maximum quantity adsorbed for Pb (II) ion onto MDP was 84.27 (mg/g) at 800 (mg/L) of adsorbate concentration. It was observed from Fig. 5 that the quantity adsorbed per gram [qe mg/g] for MDP increased with increasing metal ion concentration due to the high availability of Pb (II) ion in solution as its concentration increases (Abdus-Salam *et al*., 2021a). The adsorption trend falls gently as the adsorbate concentration increases further. It is generally accepted that the mechanism for the adsorbed metal ion is related to the surface properties of activated carbons due to the saturation of active sites on the adsorbents (Habte *et al*., 2020). Similar results have been reporting by Buhari *et al*., (2020); Yunusa and Ibrahim (2019).

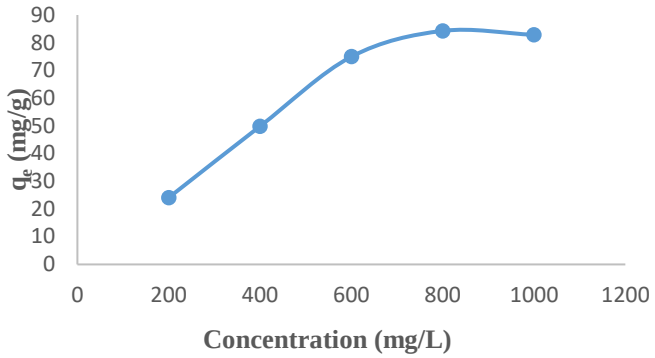

Figure 5: Effect of Initial Conc. of Pb (II) ion onto MDP Shells

Effect of Contact Time

The effect of contact time helps to understand the rate of reaction and the time the adsorption process reaches an equilibrium state (Ugbe and Ikudayisi, 2017). The effect of contact time on the adsorption of Pb (II) ion was investigated at different time intervals in the range of 30-180 min and the result was presented in Fig. 6 onto MDP. The maximum quantity adsorbed of MDP was achieved within 90 min. The adsorption took a relatively longer time to attain equilibrium due to the higher amount of adsorbate molecules that diffuse from the bulk liquid into the pores of the available number of active sites on the surface of carbons Dahri *et al*. (2014) and became slower at the later stages of contact time due to the decreased number of active sites Makeswari and Santhi (2013). Similar behaviour was observed in malachite green adsorption prepared with desert date shell (Yunusa *et al*., 2020).

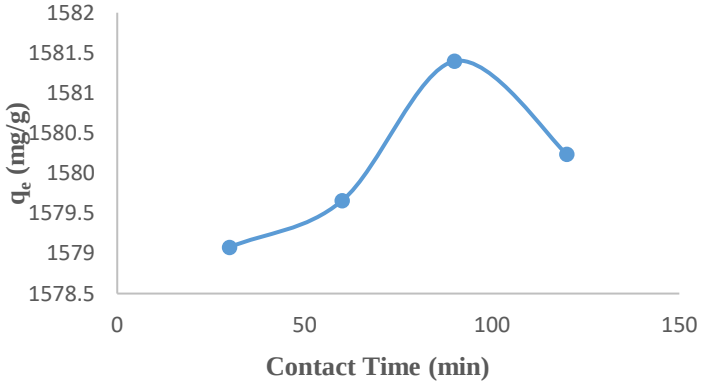

Figure 6: Effect of Contact time of Pb (II) ion onto MDP Shells

Effect of Adsorbent Dosage

To determine the minimum possible dosage for the maximum adsorption of metal ions, the amount of adsorbent dosage was varied, 0.01 g, 0.02 g, 0.03 g and 0.05 g in 100 mL of 20 ppm metal ion solution onto MDP. This experiment was conducted under optimized pH conditions of the metal ion. Fig. 7 illustrates the effect of

variation dosage on the adsorption of the metal ion. However, **t**he increment in the adsorbent dosage resulted in a declined trend in the quantity adsorbed. This may be due to the inaccessibility of the active sites or it is due to the overlapping of the adsorption sites with higher adsorbent dosage (Naeem *et al*., 2019). A similar result was also obtained from the research cited by (Zhang *et al*., 2008; (Alghamdi *et al*., 2019).

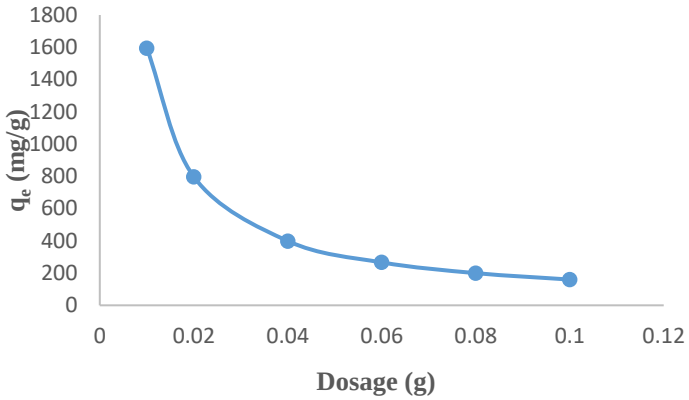

Fig. 7: Effect of Adsorbent dose of Pb (II) ion onto MDP Shells

Effect of pH

The pH of the solution has a significant effect on the uptake of metal ions since it determines the chemistry of the surface charge of the adsorbent and the degree of ionization as well as speciation of the adsorbate molecules (Gupta *et al*., 2009; Boudaoud *et al*., 2017). The pH solution governing the targeted metal ion Pb (II) ion onto MDP was presented in Fig 8. To evaluate the effect of pH on the adsorption of Pb (II) ion onto MDP was carried out with solutions with several solution pH in the range of 2-8 while keeping the other parameters constant. The result was achieved at pH 8. At a low pH value, the surface of the adsorbent is closely associated with hydroxonium H3O+ and holds the protonated active sites and maintained a net positive charge, as a result, adsorption capacity decreased. The adsorbent becomes a positive charge because of electrical repulsion between the adsorbent surface and cations. Meanwhile, lower the H+ concentration and favours adsorption by mass action. This adsorption phenomenon is subjected to bivalent cations (Ucer *et al*., 2006). The results obtained were higher than Pb^{2+}, Cd^{2+}, Cu^{2+}, and Ni^{2+} ions adsorption by Farghali *et al*. (2017).

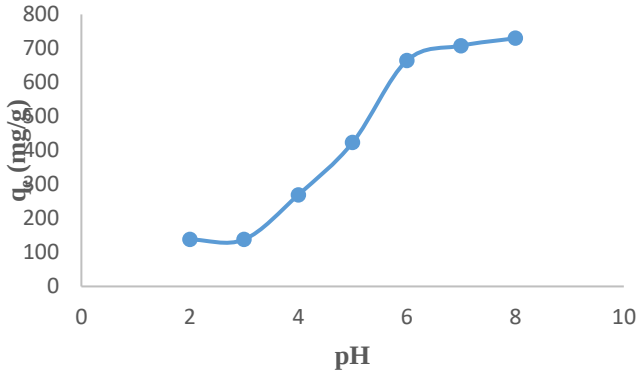

Fig. 8: Effect of pH of Pb (II) ion onto MDP Shells

Effect of Temperature

Temperature is another significant adsorption parameter as it changes the adsorption limit of the adsorbent (Goharshadi and Moghaddam, 2015). The impact of temperature on the balance takes up of Pb (II) ion onto MDP was researched at different temperatures of 40-80 ^{o}C as shown in Fig. 9. Other adsorption conditions were kept constant. The maximum quantity adsorbed was achieved at 60 ^{o}C. The effect of temperature on the adsorption of MDP shows that adsorption capacity decreases with an increase in temperature which indicates the exothermic nature of the adsorption process. The decrease in quantity adsorbed could be attributed to a decreased equilibrium constant at higher temperatures (Adegoke *et al*., 2014; Adebayo *et al*., 2016). The result obtained was higher than Cd and Pb ions reported by Akinyeye *et al*., (2020) on bamboo stem adsorption

.

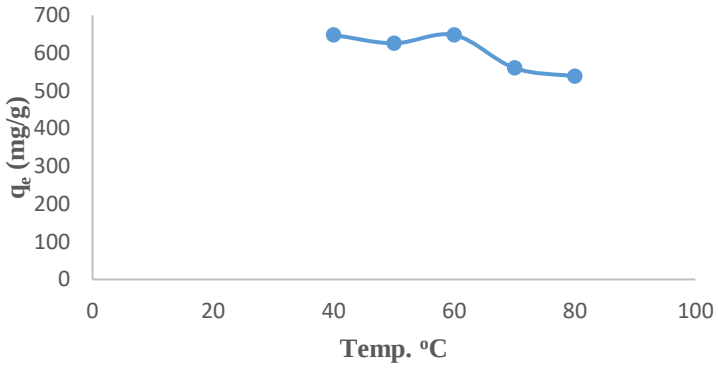

Figure 9: Effect of Temperature of Pb (II) ion onto MDP Shells

Adsorption Isotherm Models

The term Isotherm defines as the relationship between the equilibrium concentration and the amount of adsorbate adsorbed at a constant temperature. It can be described graphically how adsorbates interact with adsorbents using correlation coefficient (R^2) value to understand the conformity of the isotherm model applied to the experimental data (Dada *et al*., 2016; Yunusa and Ibrahim, 2019). The linear plots of the Langmuir, Freundlich, Temkin and Dubinin-Radushkevich (DRK) isotherm models for the adsorption of Pb (II) ion onto the MDP are presented in Figs. 10 to 13 respectively. Similarly, the summary of the adsorption isotherm parameters is presented in Table 2.

Table 2: Summary of Adsorption Isotherm parameters

Langmuir Parameter		**FreundlichParameters**		**Temkin Parameters**		**DRK Parameters**	
q_o (mg/g)	108.27	$\frac{1}{n}$	0.4994	A_T (L/mg)	0.93	q_s (mg/g)	9.54
q_m(mg/g)	103.09	n	2	b_T(J/mol)	99.98	K_{ad} (kJ^2/mol^2)	3192.9
K_L (L/mg)	38.15	K_f (mg/g)	0.181	B	24.78	E (kJ/mol)	0.0125
R_L	3.28×10^{-05}	R^2	0.8874	R^2	0.9196	R^2	0.9175
R^2	0.9506						

Langmuir isotherm

The Langmuir isotherm model generally accepted its definition as monolayer adsorption limited to an identical surface of adsorbent with no relationship between the adsorbate particles (Akinyeye *et al*., 2020). The Langmuir isotherm represents the equilibrium distribution of metal ions between the solid and liquid phases (Moosa *et al*., 2015). The Langmuir isotherm is represented in eq. (3) (Chowdhury *et al.*, 2011)

$$q_e = \frac{q_m K_L C_e}{1 + K_L C_e} \quad (3)$$

Langmuir adsorption parameters were determined by transforming the Langmuir equ. (3) into the linear form as:

$$\frac{C_e}{q_e} = \frac{1}{q_m} + \frac{1}{q_m K_L} C_e \quad (4)$$

Where, C_e = the equilibrium concentration of adsorbate (mg/L) q_e = the amount of metal adsorbed per gram of the adsorbent at equilibrium (mg/g), q_m = maximum monolayer

coverage capacity (mg/g) and K_L = Langmuir isotherm constant (mg/L).

The Langmuir parameters q_m and K_L are calculated from the slope and the intercept. It was observed from Table 2 that the adsorption data fitted best into the Langmuir isotherm model correlation coefficients (R^2) values close to unity 0.9506. Meanwhile, the correlation coefficient suggests that equilibrium data were described Langmuir isotherm model signifying a chemisorption adsorption (Hao *et al*., 2010). However, this observation was further supported by the closeness of experimental data [q_o 108.27 (mg/g)] and theoretical values [q_m103.09 (mg/g)] respectively. The closeness between the experimental data and theoretical values could be attributed to the homogenous distribution of the active sites on the surface of the adsorbents and that the adsorption indicates good monolayer coverage in nature (Abdus-Salam and Ikudayisi, 2017). Similarly, the separation factor R_L is usually employed to describe the favourability of the adsorption. It is based on the Langmuir adsorption constant:

$$K_L = \frac{1}{1 + K_L C_o} \quad (5)$$

where K_L (l/mg) is the Langmuir isotherm constant obtainable from eq. (5) and C_o (mg/L) is the initial concentration of Pb (II) ion (Dada *et al*., 2016). If $R_L > 0$ but <1 the Langmuir isotherm is favorable as in the case of this study. However, if $R_L = 1$ or 0, this type of isotherm is unfavourable or linear respectively.

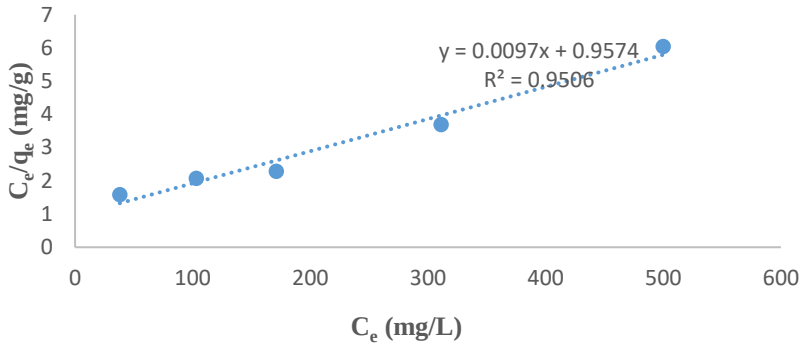

Figure 10: Langmuir Isotherm Plot for the Adsorption of Pb (II) ion onto MDP Shells

Freundlich Isotherm

The Freundlich model, (1906) is perhaps the most widely used non-linear adsorption equilibrium model which can be shown to be thermodynamically rigorous for adsorption on heterogeneous surfaces (Mansouriieh *et al*., 2016). These data often fit the empirical equation proposed by Freundlich:

$$q_e = K_f C_e^{\frac{1}{n}} \quad (6)$$

Where K_f= Freundlich isotherm constant (mg/g), C_e = the equilibrium concentration of adsorbate (mg/L), q_e= the amount of metal adsorbed per gram of the adsorbent at equilibrium (mg/g) and n =adsorption intensity. The logarithmic form of the equation (6) becomes:

$$\log q_e = \log K_f + \frac{1}{n} \log C_e \quad (7)$$

The constants K_f *and* n are Freundlichconstant characteristics of the system. The Freundlich parameters $\log K_f$ and $\frac{1}{n}$are calculated from the slope and intercept (Dada *et al*., 2012). The summary Freundlich parameters of Pb (II) ion onto MDP was presented in Table 2. It can be observed clearly from Table 2 that MDP fitted well into the Freundlich isotherm model with correlation coefficients (R^2) value 0.8874 close to unity. The MDP fitted well into Freundlich isotherm which means that it is said to be multilayer in nature (Boudaoud *et al*., 2017). The Freundlich isotherm constants K_f and n indicate adsorption capacity and intensity respectively. When the value of n lies between one and ten and $\frac{1}{n}$ being less than unity, they are said to be true reflections of favourable and normal adsorption onto MDP (Ghasemi *et al*., 2014).

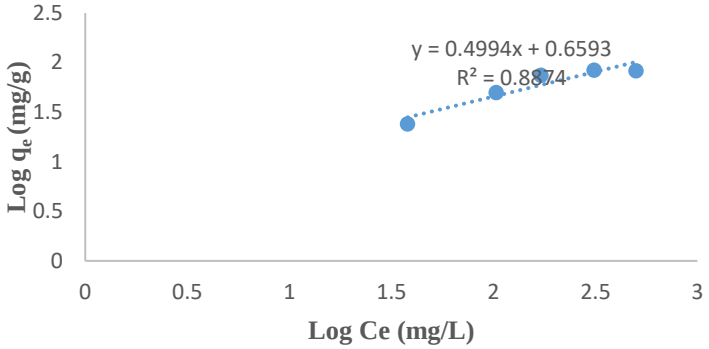

Fig. 11: Freundlich Isotherm Plot for the Adsorption of Pb (II) ion onto MDP Shells

Temkin Isotherm

The Temkin adsorption isotherm contains a factor that considers the interaction between adsorbates. The model assumes that the heat of adsorption of all molecules in the layer will decrease linearly rather than logarithmically with coverage at average concentrations. The heat of adsorption is characterized by a uniform distribution of binding energies between adsorbent and adsorbate (Edet and Ifelebuegu, 2020). The model is given by the following equations:

$$q_e = \frac{RT}{b}\ln(A_T C_e) \quad (8)$$

$$q_e = \left(\frac{RT}{b}\right)\ln A_T + \left(\frac{RT}{b}\right)\ln c_e \quad (9)$$

$$B = \frac{RT}{b_T} \quad (10)$$

$$q_e = B\ln A_T + B\ln c_e \quad (11)$$

A_T = Temkin isotherm equilibrium binding constant (L/g), b_T = Temkin isotherm constant, R = universal gas constant (8.314 J/mol/K), T = Temperature at 298 K and B = Constant related to the heat of adsorption (J/mol).

It was observed from Table 3 that the fitness of Temkin isotherm was achieved on MDP Pb (II) with (R^2) values 0.9196. Apart from the information obtained from the correlation coefficient (R^2), Temkin isotherm also gives insight into the interaction between adsorbent and adsorbate from Temkin isotherm constant related to the heat of adsorption b_T (J/mol) which decreased as a result of surface coverage. Therefore, when the heat of adsorption b_T (J/mol) is less than 8 signifies that attractive forces are weak and physical in nature whereas values greater than 8 are indicative of strong and chemical interaction (Theivarasu and Mylsamy, 2010).

As reported in Table 3, the b_T (J/mol) results revealed 99.98 J/mol shows strong chemical interaction in nature. The results obtained are in agreement with the b_T and R^2 values (52.36 J/mol and 0.917) reported by Azeez and Adekola, (2016).

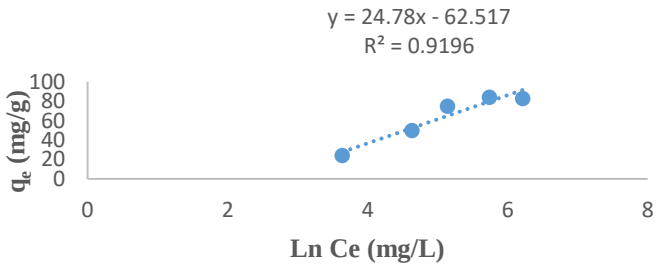

Figure 12: Temkin Isotherm Plot for the Adsorption of Pb (II) ion onto MDP Shells

Dubinin–Radushkevich Isotherm Model

Dubinin–Radushkevich isotherm is generally applied to express the adsorption mechanism with a Gaussian energy distribution onto a heterogeneous surface (Dabrowski, 2001). The model has often successfully fitted high solute activities and the intermediate range of concentrations data well.

$$q_e = (q_s)\exp(-K_{ad}\varepsilon^2) \quad (12)$$

$$\ln q_e = \ln(q_s) - (K_{ad}\varepsilon^2) \quad (13)$$

Where q_e = amount of adsorbate in the adsorbent at equilibrium(mg/g); q_s = theoretical isotherm saturation capacity (mg/g);K_{ad} = Dubinin–Radushkevich isotherm constant (mol^2/kJ^2) and ε = Dubinin–Radushkevich isotherm constant. The approach was usually applied to distinguish the physical and chemical adsorption of metal ions with its mean free energy, E per molecule of adsorbate (for removing a molecule from its location in the sorption space to infinity) can be computed by the relationship (Dubinin, 1960; Hobson, 1969):

$$E = \left[\frac{1}{\sqrt{2K_{ad}}}\right] \quad (14)$$

Where K_{ad} is denoted as the isotherm constant. Meanwhile the parameter ε can be calculated as

$$\varepsilon = RT \ln\left[1 + \frac{1}{C_e}\right] (15)$$

Where R, T *and* C_e represent the gas constant (8.314 J/mol K), absolute temperature (K) and adsorbate equilibrium concentration (mg/L), respectively. One of the unique features of the Dubinin-Radushkevich (DRK) isotherm model lies in the fact that it is temperature-dependent, which is when adsorption data at different temperatures are plotted as a function of the logarithm of the amount adsorbed ($\ln q_e$) versus ε^2 the square of potential energy, all suitable data will lie on the same curve, named as the characteristic curve (Foo and Hameed, 2010; Dada *et al*., 2012).

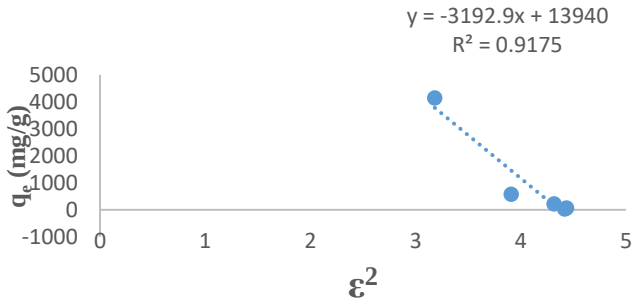

Fig. 13: Dubinin–Radushkevich Isotherm Plot for the Adsorption of Pb (II) ion onto MDP Shells

Adsorption Kinetics Models

The adsorption kinetics provides the rate of adsorbate uptake onto the activated adsorbent within the equilibrium contact time (Danmallam *et al*., 2020). The Pseudo-first order, Pseudo-second order kinetic models, Intra-particle diffusion and Elovich adsorption kinetic models were implemented to evaluate the rate constant of the adsorption process. The linearity of the plots with correlation coefficient values (R^2) that are very close to unity is an indication that the adsorption process followed any of the aforementioned kinetic models (Abdus-Salam and Buhari, 2016). The summary of the kinetic parameters for Pseudo-first order, second order, Intra-particle diffusion and Elovich models are shown in Table 3 for Pb (II) ion onto MDP. The plots of Pseudo-first order, second order, Intra-particle diffusion and Elovich models of the above-mentioned models are presented in Figs. 14 – 17 respectively.

Table 3: Summary of Kinetic Models Parameters

Pseudo-first order		**Pseudo-second order**		**Intra-Particle Diff.**		**Elovich**	
K_1 (min^{-1})	2.16×10^{-2}	K_2 (g/mg/min)	2.83×10^{-03}	k_i (mg/g/min^2)	0.2158	α(mg/g/min^2)	4.58×10^{-2}
$q_{e\ exp}$ (mg/g)	84.27	$q_{e\ exp}$ (mg/g)	84.27	C	-10.746	β(mg/g/min)	129.87
q_{ecal} (mg/g)	23.33	q_{ecal} (mg/g)	88.49	R^2	0.6	R^2	0.1244
R^2	0.2987	R^2	0.9875				

Pseudo-first order Kinetics

The linear form of Pseudo-first-order kinetic model described by Lagergren, (1898) is expressed by the following equation:

$$In\,(q_e - q_t) = In\,q_e - k_1 t \qquad (16)$$

where q_e and $q_t$are the values of the amount adsorbed per unit mass at equilibrium and at any time t. The values of k_1 can be obtained in the slope of the linear plot of $In\,(q_e - q_t)$vs. t.

It was observed from Table 3 that the adsorbent with the pseudo-first-order kinetic model on the fact that its correlation coefficient value (R^2) was close to unity (0.909). However, the q_e calculated differs significantly with the q_e experimental on the tested. This could be related to the rate controlling the steps for the uptake of ions is resistance to the boundary layer (Akinyeye *et al*., 2020). These results were in agreement with the literature reported by Ghasemi *et al*. (2014).

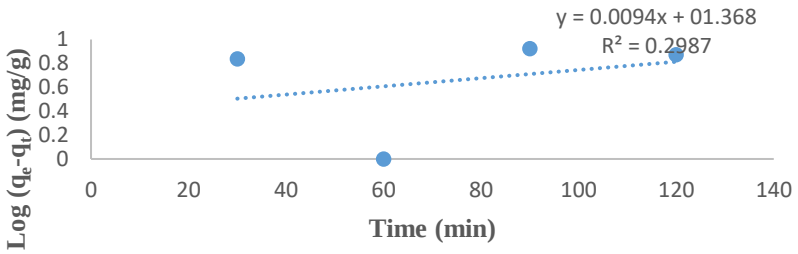

Figure 14: Pseudo-first Order Plot for the Adsorption of Pb (II) ion onto MDP Shells

Pseudo-second-order Kinetics

Generally speaking, the pseudo-second-order kinetic model is the rate-limiting step of chemisorption involving forces sharing or exchange of electrons between the adsorbate and the adsorbent (Akinyeye *et al*., 2020). The adsorption parameters derived from the pseudo-second-order kinetic model of Pb (II) ion onto MDP were summarized in Table 3.

The linear form as described by Ho and McKay, (1998) is represented by the following equation:

$$\frac{t}{q_t} = \frac{1}{\left(\frac{1}{k_e q_e^2}\right) + \left(\frac{1}{q_e}\right) \cdot t} \qquad (17)$$

Where k_2 is the second order rate coefficient (g/min/mg), q_e is the equilibrium amount of adsorbate adsorbed per unit mass of the adsorbent (mg/g), q_t, is the amount of adsorbate adsorbed per unit mass of adsorbent at time t (mg/g), and t is the time (min). The equilibrium adsorption capacity (q_e), and the constant K_2 can be obtained from the slope and intercept of a plot $\frac{t}{q_t}$ against t.

It can be seen from Table 3 that the degree of correlation coefficient (R^2) is found to be extremely high with a value close to unity (1). It could be concluded that the adsorbent

fitted perfectly well into the pseudo-second-order kinetic model because of the strong interaction between the adsorbent and the adsorbate (Adebayo *et al*., 2016). However, the q_e calculated of MDP was significantly higher than the q_e experimental values of the pseudo-second-order model. This variation could be attributed to adsorbate and adsorbent interaction, transfer of adsorbent particle surface to the intra-particle active sites or intra-particle precipitation phenomena (Akinyeye *et al*., 2020). The results obtained are in agreement with the observation reported by Akinyeye *et al*. (2020); Dada *et al*. (2016).

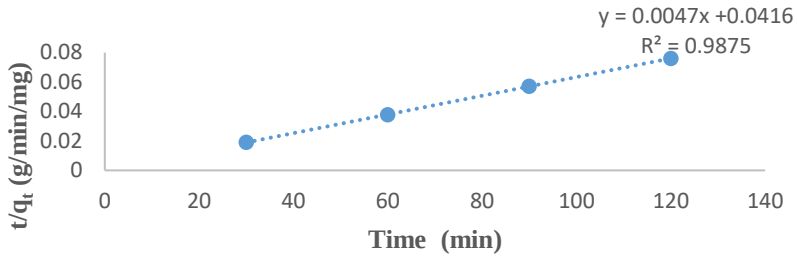

Figure 15: Pseudo-second Order Plot for the Adsorption of Pb (II) ion onto MDP Shells

Intra-particle Diffusion Kinetic

The intra-particle diffusion kinetic model assumes that solubilized metal ions transport from the aqueous medium to the adsorbent materials then an intra-particle diffusion assay takes place (Mohamed *et al*., 2019). The values of R^2 (correlation coefficient) are taken into consideration as a measure of the applicability and goodness of fit of the experimental data obtained from the slope of the plot q_t vs $t^{1/2}$. The intra-particle diffusion equation is given (Cheung *et al*., 2007):

$$q_t = k_i\, t^{1/2} + C \quad (18)$$

where q_t is the amount of solute on the surface of the sorbent at time t (mg/g) and k_i is the intraparticle diffusion rate constant (mg/g $min^{1/2}$).

It can be observed from Table 3 that the R^2 value was found to be 0.0802 which is far from unity. Similarly, the rate constant of pore diffusion K_i value was found to be 0.174 ($mg/g/min^2$) which rules out the diffusion kinetics. The bulk diffusion is the important aspect attributed to the initial linear portion meanwhile; equilibrium is represented by the plateau portion and intra-particle diffusion when it passes through the origin (Nwosu *et al*., 2019). The corporality of linear relationship between amount q_e against $t^{1/2}$ signifies that intra-particle diffusion partake during the adsorption process. If the straight line of the plot of q_e against $t^{1/2}$ went through the origin, then intra-particle diffusion becomes the controlling step. However, if the straight line does not pass through the origin, it indicates that the intra-particle diffusion is not the only controlling step but that boundary surface effects are also involved (Nwosu *et al*., 2017).

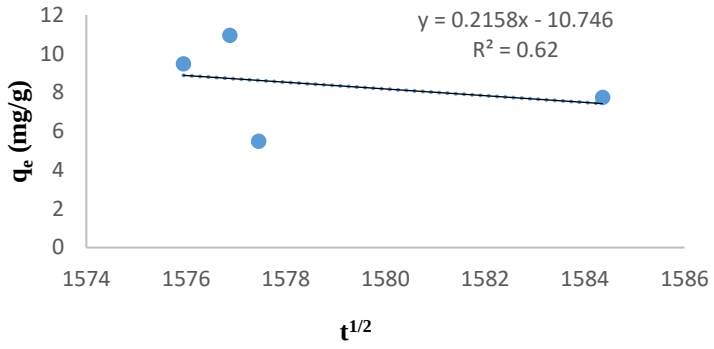

Figure 16: Intra-particle Diffusion Plot for the Adsorption of Pb (II) ion onto MDP Shells

Elovich Model

The Elovich equation assumes that the actual solid surfaces are energetically heterogeneous. Such an assumption is obvious because neither desorption nor interactions between the adsorbed molecules could substantially affect the kinetics of adsorption at low surface coverage. The crucial effect of the surface energetic heterogeneity on the equilibria of adsorption in the gas/solid systems has been demonstrated by (Dada *et al*., 2016). The Elovich Equation (Ho and McKay, 1998; Abdel-Salam *et al*., 2014) has been used in the form of;

$$\frac{dq_t}{dt} = \alpha \exp -\beta q_t \quad (19)$$

Assuming $\alpha\beta t >> 1, q_t = 0\ at\ t = 0\ and\ q_t = q_t\ at\ t = t$, the linear form of the equation (19) is given by (Ho and McKay, 1998):

$$q_t = \beta\ In\ (\alpha\beta) + \beta In\ t \quad (20)$$

where $\alpha\ and\ \beta$ are the Elovich coefficients, represent the initial adsorption rate (g $mg^{-1}min^{-2}$) and the desorption coefficient (mg $g^{-1}min^{-1}$) respectively. The Elovich coefficients could be computed from the plots of q_t vs. ln t. It can be seen in Fig. 16 that the linear correlation coefficient was found to be 0.0467. It can be deduced that the data obtained did not fit well into Elovich model.

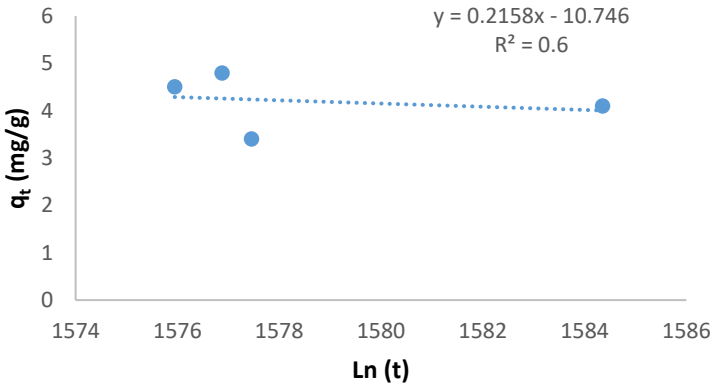

Fig. 17: Elovich Plot for the Adsorption of Pb (II) ion onto MDP Shells

Thermodynamic Studies

Thermodynamics is used to determine if the process is spontaneous or not (Ho and Ofomaja, 2006). Thermodynamic parameters were determined following experiments in the temperature range of 313–353 K. Generally, the heterogeneous equilibrium constant K_c for the adsorption equilibria is given by the equation:

$$K_c = \frac{C_s}{C_e} \quad (21)$$

where C_s (mg/L) is the amount of adsorbate in the liquid phase and C_e (mg/L) is the equilibrium concentration of Pb (II) ion adsorption onto MDP respectively. Other thermodynamic parameters including Gibbs free energy (ΔG^o), standard enthalpy change (ΔH^o) and standard entropy change (ΔS^o) were evaluated using the following equations:

$\Delta G^o = - RT\ln K_c$ (22)

where R (8.314 J mol^{-1} K^{-1}) is the universal gas constant, T (K) is the temperature, and Kc is the equilibrium constant of adsorption which were determined by Van't Hoff equation:

$$\ln K_c = -\frac{\Delta H^\circ}{RT} + \frac{\Delta S^\circ}{R} \quad (22)$$

where the values ΔS^o and ΔH^o can be estimated from the slope and intercept of plot of ΔG against T, respectively as shown in Fig. 18.

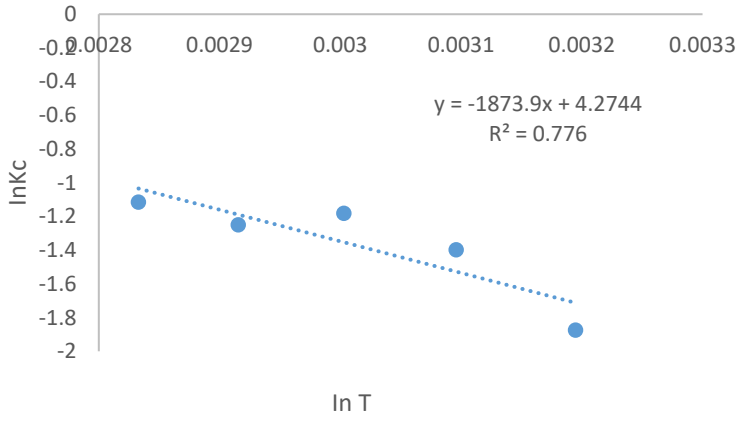

Fig. 18: Van't Hoff Plot for the Adsorption of Pb (II) ion onto MDP Shells

The values of thermodynamic parameters for Pb (II) ion adsorption onto MDP have been summarized in Table 4. The negative values of ΔGo indicated that the adsorption process is a feasible and spontaneous reaction and decreased in their absolute values with temperature (Abdus-Salam *et al*., 2021a). Similarly, the negative value of ΔH confirms the exothermic nature of the adsorption and the system is energetically stable at the given temperature (Adegoke *et al*., 2014; Nwosu *et al*., 2019). However, the entropy change is positive (+ΔS), and there's an increased in the degree of randomness at the solid-solution interface during the adsorption process. This was also observed by (Dada *et al*., 2016; Abdus-Salam *et al*., 2021b).

Table 4: Thermodynamic parameters of Pb (II) ion onto MDP

ΔH (kJ/mol)	ΔS (kJ/mol/k)	ΔG°(kJ/mol)				
-15.5796	0.03554	313°K	323°K	333°K	343°K	353°K
		-26.7036	-27.059	-27.4144	-27.7698	-28.1252

CONCLUSION

The present study evaluates the efficacy of a modified Doum palm shell as an effective, promising and available adsorbent for the removal of Pb (II) ion from an aqueous medium. It could be concluded that the modified Doum palm shell activated with 2 M 1:2 ZnCl2 has a good adsorbing performance for the removal of lead. The adsorption of Pb (II) ion was found to be maximum at 800 mg/L initial concentration, adsorbent dosage 0.01 g, pH of 8 and 90 min contact time. The adsorption isotherms fitted best in the following order Langmuir > Temkin > DRK > Freundlich. The adsorption of the Pb (II) ion onto the modified Doum palm shell follows a pseudo-second-order kinetic model with a high correlation coefficient (R2) value. The thermodynamic studies revealed that the adsorption was exothermic in nature, spontaneous and feasible. Therefore, an MDP shell is recommended as an available, effective and potential adsorbent for the adsorption of Pb (II) ion removal in wastewater.

ACKNOWLEDGEMENT

The authors are grateful to Prof. N. Abdus-Salam, Faculty of Physical Sciences, Department of Chemistry, University of Ilorin, Nigeria for providing enabling research environment. Also acknowledged the ***ASTD TETFund*** (2018) for the financial support of my PhD programme.

COMPETING INTEREST

The authors have declared that no competing interests exist.

REFERENCES

Abdus-Salam, N., Ikudayisi-Ugbe, A. V. and Ugbe, F. A. (2021a). Adsorptive Removal of Methylene Blue from Synthetic Wastewater Using Date Palm Seeds, Goethite and their Composite. *Acta Scientifica Malaysia (ASM)*, 1: 27-35.

Abdus-Salam, N., Ikudayisi, V. A. and Ugbe, F. A. (2021b). Adsorption studies of acid dye-Eosin yellow on date palm seeds goethite and their composite. *Chemical data collections*, 31: 100626

Abdus-Salam, N. Adekola, S. K. (2018). Adsorption studies of zinc(II) on magnetite, baobab (*Adansonia digitata*) and magnetite–baobab composite. *Applied Water Science, 8*: 222

Abdus-Salam, N. and Bello, M. O. (2015). Kinetics, thermodynamics and competitive adsorption of lead and zinc ions onto termite mound. *International Journal of Environmental Science and Technology*, *12*:3417–3426

Abdus-Salam, N. and Buhari, M. (2014). Adsorption of Alizarin and Fluorescein Dyes on Adsorbent prepared from

Mango Seed. *The Pacific Journal of Science and Technology,15*:232-235

Abdus-Salam, N. and Buhari, M. (2016). Adsorption of Alizarin and Fluorescein Dyes onto Palm Seeds Activated Carbon: Kinetic and Thermodynamic Studies. *Journal of the Chemical Society of Pakistan, 38*: 604-612

Abdus-Salam, N. and Ikudayisi, V. A. (2017). Preparation and characterization of synthesized goethite and goethite-date palm seeds charcoal composite. *Ife Journal of Science,19*: 99-107

Abu-Elalla, F. M. (2009). Antioxidant and anticancer activities of Doum fruit extract (*Hyphaene thebaica*) *African Journal of Pure and Applied Chemistry, 3*:197-201

Adebayo, G. B., Abdus-Salam, N. and Alimi, E. S. (2014). Adsorption of Lead (II) ions by Activated Carbon prepared from different parts of *Jatropha Curcas* Plant. Publication of faculty of science, Unilorin, *Ilorin Journal of Science, 1*:28-49

Adebayo, G. B., Mohammed, A. A. and Sokoya, S. O. (2016). Biosorption of Fe (II) and Cd (II) ions from aqueous solution using a low cost Adsorbent from Orange Peels. *Journal of Applied Science and Environmental Management, 20*:702-714

Adegoke, H. I., Adekola, F. A. and Abdulraheem, M. N. (2017). Kinetic and thermodynamic studies on adsorption of sulphate from aqueous solution by magnetite, activated carbon and magnetite-activated carbon composites. *Nigerian Journal of Chemical Research, 22*: 39-65

Adegoke, I. A., Adekola, F. A., Fatoki, O. S. and Ximba, B. J. (2014). Adsorption of Cr (VI) on synthetic hematite (alpha-Fe_2O_3) nanoparticles of different morphologies. *Korean Journal of Engineering, 31:* 142-152

Adekola, F. A., Abdus-Salam, N., Adegoke, H. I., Adesola, A. M., and Adekeye, J. I. D. (2012). Removal of Pb (II) from aqueous solution by natural and synthetic calcites. *Bulletin of Chemical Society of Ethiopia, 26*:195-210

Akinyeye, O. J., Ibigbami, T. B., Odeja, O. O. and Sosanolu, O. M. (2020). Evaluation of kinetics and equilibrium studies of biosorption potentials of bamboo stem biomass for removal of Lead (II) and Cadmium (II) ions from aqueous solution. *African Journal of Pure and Applied Chemistry, 14*: 24-41

Alghamdi, A. A., Al-Odayni, A. B., Saeed, W. S., Al-Kahtani, A., Alharthi, F. A. and Aouak, T. (2019). Efficient adsorption of lead (II), from aqueous phase solutions using polypyrrole-based activated carbon. *Materials, 12:* 20-29

Ayob, S., Othman, N., Altowayti, W. A. A., Khalid, F. S., Abu-Bakar, N., Tahir, M., and Soedjono, E. S. (2021). A Review on Adsorption of Heavy Metals from Wood-Industrial Wastewater by Oil Palm Waste. *Journal of Ecological Engineering, 3:* 249–265

Azeez, S. O. and Adekola, F. A. (2016). Sorption of 4-Nitroaniline on Activated Kaolinitic Clay and Jatropha curcas Activated Carbon in Aqueous Solution. *Pakistan Journal of Analytical and Environmental Chemistry, 17*:105-145

Babarinde, A., Ogundipe, K., Sangosanya, K. T., Akintola, B. D. and Hassan, A. O. E. (2016). Comparative study on the biosorption of Pb(II), Cd(II) and Zn(II) using lemon grass (Cymbopogon citratus): kinetics, isotherms and thermodynamics. *Chemistry International 2*: 89-102

Boudaoud, A., Djedid, M., Benalia, M., Chifaa, A., Bouzar, N. and Elmsellem, H. (2017). Removal of Nickel (II) and Cadmium (II) ions from wastewater by Palm Fibers. *Scientific Study and Research Journal, 18:* 391-406

Buhari M., Maigari, A. U., Abubakar, U. A., Sani, M. M. and Maigari, A. U. (2020). Batch Adsorption of Safranin Dye from an Aqueous Solution of *Balanites aegyptiaca* Seed Coats. *Asian Journal*

of Physical and Chemical Sciences, 8: 48-54

Cheung, W. H., Szeto, Y. S. and McKay, G. (2007). Intra-particle diffusion processes during acid dye adsorption onto chitosan. *Bioresources Technology, 98*: 2897–2904

Dąbrowski, A. (2001). Adsorption from theory to practice. *Advances in Colloid and Interface Science,93*: 135–224

Dada, A. O., Inyinbor, A. A., Idu, E. I., Bello, O. M., Oluyori, A. P., Adelani-Akande, T. A., Okunola, A. A. and Dada, O. (2018). Effect of operational parameters, characterization and antibacterial studies of green synthesis of silver nanoparticles using Tithonia diversifolia. *Peer Journal, 10*: 1-17

Dada, A. O., Latona, D. F., Ojediran, O. J. and Nath, O. O. (2016). Adsorption of Cu (II) onto Bamboo Supported Manganese (BS-Mn) Nanocomposite: Effect of Operational Parameters, Kinetic, Isotherms, and Thermodynamic Studies, *Journal Applied Science and Environmental Management, 20*: 409-422

Dada, A. O., Olalekan, A. P., Olatunya, A. M. and Dada, O. (2012). Langmuir, Freundlich, Temkin and Dubinin–Radushkevich Isotherms Studies of Equilibrium Sorption of Zn^{2+} Unto Phosphoric Acid Modified Rice Husk. *Journal of Applied Chemistry,* 3: 38-45

Dahri, M. K., Kooh, M. R. R. and Lim, L. B. L. (2014). Water Remediation Using Low Cost Adsorbent Walnut Shell for Removal of Malachite Green: Equilibrium, Kinetics, Thermodynamic and Regeneration Studies. *Journal of Environmental Chemical Engineering, 2*: 1434–1444

Danmallam, A. A., Dabature, W. L., Pindiga, N. Y., Magaji, B., Aboki, M. A. Ibrahim, D., Zanna, U. A. S. and Muktar, M. S. (2020). The Kinetics of the Adsorption Process of Cr (VI) in Aqueous Solution Using Neem Seed Husk (*Azadirachta indica*) Activated Carbon. *Physical Science International Journal, 24*: 1-13

Dubinin, M. M. (1960). The Potential Theory of Adsorption of Gases and Vapors for Adsorbents with Energetically Non-uniform Surfaces. *Chemical Reviews, 2*: 235–241

Edet, U. A. and Ifelebuegu, A. O. (2020). Kinetics, Isotherms, and Thermodynamic Modeling of the Adsorption of Phosphates from Model Wastewater Using Recycled Brick Waste. *Processes, 8:* 1-15

EPA (2021). Environmental protection Agency. Safe Drinking Water. National Primary Drinking Water Regulations. National Secondary Drinking Water Regulation. visit: epa.gov/safewater

Farghali, A. A., Tawab, H. A. A., Moaty, A. M. and Khaled, R. (2017). Functionalization of acidified multi-walled carbon nanotubes for removal of heavy metals in aqueous solutions. *Journal of Nanostructure Chemistry, 7:* 101–111

Freundlich, H. (1906). Adsorption in solutions. *Physical Chemistry, 57*: 385 –470

Foo, K.Y. and Hameed, B. H. (2010). Insights into the modelling of adsorption isotherm systems, *Review Chemical Engineering Journal, 6*: 2–10

Gaya, U. I., Otene, E. and Abdullah, A. H. (2015). Adsorption of aqueous Cd (II) and Pb (II) on activated carbon nanopores prepared by chemical activation of Doum palm shell. *Springer Plus, 4:* 1-18

Ghasemi, M., Naushad, M., Ghasemi, N. and Khosravi-Fard, Y. (2014). Adsorption of Pb (II) from aqueous solution using new adsorbents prepared from agricultural waste: Adsorption isotherm and kinetic studies. *Journal of Industrial and Engineering Chemistry, 20:* 2193-2199

Goharshadi, E. K. and Moghaddam, M. B. (2015). Adsorption of hexavalent chromium ions from aqueous solution by graphene nanosheets: kinetic and thermodynamic studies. *International Journal Environmental Science and Technology, 12:* 2153–2160

Gupta, V. K., Carrott, P. J. M., Ribeiro-Carrott, M. M. L. and Suhas, T. L. (2009). Low-cost adsorbents: growing approach to wastewater treatment. *Critical Review. Environmental Science Technology, 39*: 783–842

Habte, L., Shiferaw, N., Khan, M. D., Thriveni, T. and Ahn, J. W. (2020). Sorption of Cd^{2+} and Pb^{2+} on Aragonite Synthesized from Eggshell. *Sustainability, 12*: 1-15

Hao, Y. M., Chen, M. and Hu, Z. B. (2010). Effective removal of Cu (II) ions from aqueous solution by amino functionalized magnetic nanoparticles, *Journal of Hazardous Materials, 184*: 392–399

Ho, Y. S. and McKay, G. (1998). Sorption of dye from aqueous solution by peat. *Chemical Engineering Journal, 2*: 115-124

Ho, Y. S. and Ofomaja, A. E. (2006). Biosorption thermodynamics of Cadmium on coconut copra meal as biosorption. *Biochemical Engineering Journals, 2*:117-123

Hobson, J. P. (1969). Physical adsorption isotherms extending from ultra-high vacuum vapour pressure. *Journal of Physical Chemistry, 8*: 2720-2727

Lagergren, S. (1898). About the theory of so-called adsorption of soluble substances. *Kungliga Svenska Vetenskapsakademiens Handlingar, 24*: 1-39

Langmuir, I. (1918). The adsorption of gases on plane surfaces of glass, mica and platinum. *Journal of American Chemical Society, 40*: 1362-1403

Ltifi, I., Ayari F., Hassen-Chehimi, D. B. and Ayadi, M. T. (2017). Study of the Adsorption of Bright Green by a Natural Clay and Modified. *Journal of Material Sciences and Engineering, 6*: 1-7

Mafra, M. R., Igarashi-Mafra, L., Zuim, D. R., Vasques, É. C. and Ferreira, M. A. (2013). Adsorption of Remazol Brilliant Blue on an Orange Peel Adsorbent. *Brazilian Journal of Chemical Engineering, 30*: 657-665

Mahdavian, L. (2012). Effects of magnetic field, pH and retention time on the lead (Pb^{2+}) adsorption by modified human hair, goat hair and sheep wool. *African Journal of Microbiology Research, 6*: 183-189

Makeswari, M. and Santhi, T. (2013). Optimization of preparation of activated carbon from Ricinus communis Leaves by microwave-assisted Zinc Chloride chemical activation: Competitive Adsorption of Ni^{2+} ions from aqueous solution. *Journal of Chemistry, 10*: 1-12

Mansouriieh, N., Sohrabi, M. R. and Khosravi, M. (2016). Adsorption kinetics and thermodynamics of organophosphorus profenofos pesticide onto Fe/Ni bimetallic nanoparticles. *International Journal of Environmental Science and Technology, 13*: 1393–1404

Mohamed, H. S. Soliman, N. K., Abdelrheem, D. A., Ramadan, A. A., Elghandour, A. H. and Ahmed, S. A. (2019). Adsorption of Cd^{2+} and Cr^{3+} ions from aqueous solutions by using residue Podinagymnospora waste as promising low-cost adsorbent, *Heliyon, 5*: 1-16

Moosa, A. A., Ridha, A. M. and Abdullha, I. N. (2015). Chromium ions Removal from Wastewater using Carbon Nanotubes. *International Journal of Innovative Research in Science, Engineering and Technology, 4*: 275-282

Naeem, M. A., Imran, M., Amjad, M., Abbas, G., Tahir, M., Murtaza, B., Zakir, A., Shahid, M., Bulgariu, L. and Ahmad, I. (2019). Batch and Column Scale Removal of Cadmium from Water Using Raw and Acid Activated Wheat Straw Biochar. Water, 11: 14-38

Nwosu, F. O. Dosumu, O. O. and Okocha, J. O. (2008). *The Potential of Terminalia catappa* (Almond) *and Hyphaene thebaica* (Doum palm) Fruits as Raw Materials for Livestock feed. *African Journal of Biotechnology*, 7: 4576-4580

Nwosu, F. O., Adekola, F. A. and Salami, A. O. (2017). Adsorption of 4-Nitrophenol Using Pilli Nut Shell Active Carbon.

Pakistan Journal of Analytical and Environmental Chemistry, 18: 69–83

Nwosu, F. O., Ajala, O. J., Okeola, F. O., Adebayo, S. A., Olankun, O. K. and Eletta, A. O. (2019). Adsorption of chlorotriazine herbicide onto unmodified and modified kaolinite: Equilibrium, kinetic and thermodynamic studies. *Egyptian Journal of Aquatic Research, 45:* 99-107

Nyijime, T. A., Ayuba, A. M. and Chahu, H. F. (2021). Removal of Pendimethalin from Aqueous Solution by Carbon prepared from Bambara Groundnut (*vigna subteranean*) Shells. *Arabian Journal of Chemical and Environmental Research*, 8: 315–335

Ombugus, M. W., Ahulle, W. R., Adams, I. U. and Shaibu, E. I. (2021). Human Health Risks of Heavy Metal in Wells and Streams Water in the Vicinity of a Lead Mining in Nasarawa State, North Central, Nigeria. *Journal of Health and Environmental Research, 2:* 76-87

Salih, O. M. (1991). *Biochemical and Nutritional Evaluation of Famine Foods of the Sudan.* Ph.D thesis Faculty of Agriculture, University of Khartoum, Sudan

Song, D., Pan, K., Tariq, A., Azizullah, A., Zilong, S., Li, Z. and Xiong, Q. (2016). Adsorptive Removal of Toxic Chromium from Waste-Water Using Wheat Straw and *Eupatorium adenophorum. PLoS ONE, 12:* 1-15

Thievarasu, C. and Mylsamy, S. (2010). Equilibrium and kinetic adsorption studies of Rhodamine-B from aqueous solution using cocoa (*Theobroma cocoa*) shell as a new adsorbent. *International Journal of Engineering Science Technology, 2*: 6284-6292

Tóth, G., Hermann, T., Da-Silva, M. R. and Montanarella L (2016). Heavy metals in Agricultural soils of the European Union with implication for food safety. *Environment International Journal 88:*299-309

Ucer, A., Uyanik, A. and Aygun, S. (2006). Adsorption of Cu (II), Cd (II), Zn (II), Mn (II) and Fe (III) ions by tannic acid immobilised activated carbon. *Separation and Purification Technology, 47:* 113–118

Ugbe, F. A. and Ikudayisi, V. A. (2017). The kinetics of eosin yellow removal from aqueous solution using pineapple peels. *Edorium Journal of Waste Management, 2*: 5–11

Wang, C. C., Si, L. F., Guo, S. N. and Zheng, J. L. (2019). Negative effects of acute cadmium on stress defense, immunity, and metal homeostasis in liver of zebrafish: The protective role of environmental zinc pre-exposure. *Chemosphere, 222:*91-97

World Health Organization (WHO) (2016). *Lead poisoning and health*. Archived from the original on 18 October 2016. Retrieved 14 October 2016

Yunusa, U., Usman, B. and Ibrahim, M. B. (2020). Kinetic and thermodynamic studies of malachite green adsorption using activated carbon prepared from desert date seed shell. *Algerian Journal of Engineering and Technology, 2*: 1-10

Yunusa, U. and Ibrahim, M. B. (2019). Reclamation of Malachite Green-Bearing Wastewater Using Desert Date Seed Shell: Adsorption Isotherms, Desorption and Reusability Studies. *ChemSearch Journal, 2*: 112 – 122

Zhang, J., Li, Y., Zhang, C. and Jing, Y. (2008). Adsorption of malachite green from aqueous solution onto carbon prepared from *Arundo donax root*. *Journal of Hazardous Materials, 150*: 774-782